Clim. Past Discuss., 9, 5521–5551, 2013
www.clim-past-discuss.net/9/5521/2013/
doi:10.5194/cpd-9-5521-2013

Climate of the Past
Discussions
Open Access

Migrating subtropical front and Agulhas Return Current affect the southwestern Indian Ocean during the late Quaternary

D. K. Naik[1], **R. Saraswat**[1], **N. Khare**[2], **A. C. Pandey**[3,*], **and R. Nigam**[1]

[1]Micropaleontology Laboratory, National Institute of Oceanography, Goa, India
[2]Ministry of Earth Sciences, New Delhi, India
[3]Allahabad University, Allahabad, India
[*]now at: Bundelkhand University, Jhansi, India

Received: 14 August 2013 – Accepted: 16 September 2013 – Published: 30 September 2013

Correspondence to: R. Saraswat (rsaraswat@nio.org)

Published by Copernicus Publications on behalf of the European Geosciences Union.

Abstract

The position of sub-tropical front (STF), Agulhas Current (AC) and Agulhas Return Current (ARC) controls the hydrography of southwestern Indian Ocean. Although, equatorward migration of STF and reduction in Agulhas leakage has been reported during the last glacial period, the fate of ARC during the last glacial–interglacial cycle is not clear. Therefore, in order to understand changes in the position and strength of ARC during the last glacial–interglacial cycle, here we reconstruct hydrographic changes in the southwestern Indian Ocean from temporal variation in planktic foraminiferal abundance, stable isotopic ratio ($\delta^{18}O$) and trace metal ratio (Mg/Ca) of planktic foraminifera *Globigerina bulloides* in a core collected from the Agulhas Retroflection Region (ARR) in the southwestern Indian Ocean. Increased abundance of *G. bulloides* suggests that the productivity in the southwestern Indian Ocean increased during glacial period which confirms previous reports of high glacial productivity in the Southern Ocean. The increased productivity was likely driven by a combination of equator-ward migration of subtropical front and westerlies. Increase in relative abundance of *Neogloboquadrina pachyderma* Dextral suggests warming of ARR leading to strong thermocline in the southwestern Indian Ocean during the last glacial period. We suggest that the warming of Agulhas Retroflection Region was driven by strengthened ARC which shifted to the east of its present location, thus bringing warmer and saltier water to the southwestern Indian Ocean. Therefore, it is inferred that over the last glacial–interglacial cycle, the hydrography of southwestern Indian Ocean was driven by an eastward shift of retroflection region as well as migrating subtropical front.

1 Introduction

The southwestern Indian Ocean is the conduit for transport of about 70 Sv of warm and salty water from the Indian Ocean into the Atlantic Ocean, via the eddy shedding by the Agulhas Current (AC) (Gordon, 1986; Bryden and Beal, 2001; Beal et al., 2011).

A part of the AC, retroflects off the southern tip of Africa and returns back to the Indian Ocean as Agulhas Return Current (ARC) (Quartly and Srokosz, 1993; Lutjeharms and Ansorge, 2001; Quartly et al., 2006). The retroflection depends on the inertia of the AC off Africa, wind stress over this region and the bottom topography (Lutjeharms and Ballegooyen, 1988; Le Bars et al., 2012). A distinct seasonality in Agulhas Retroflection (AR) is also observed with early retroflection during austral summer than in winter (Matano et al., 1998). A few sporadic large eastward shifts of the AR, leading to disruption of eddy shedding and thus reduction in the amount of water being transported from the south Indian to the south Atlantic Ocean have also been observed (van Aken et al., 2013). A significant change in this inter-ocean water exchange has also been reported over the geologic period (Rau et al., 2002), especially the glacial terminations (Peeters et al., 2004; Barker et al., 2009). As the global thermohaline circulation responds to the changes in amount of water transported from the Indian and Pacific Ocean to the south Atlantic via the Agulhas Current in the southwestern Indian Ocean (Knorr and Lohmann, 2003; Beal et al., 2011), it is possible that the changes in the southwestern Indian Ocean may be a precursor to climate changes over the North Atlantic (de Ruijter et al., 2005). The strength of the ARC depends on the retroflection as well as the position of sub-tropical front (STF), which marks the transition between tropical Indian Ocean and the Southern Ocean, and is distinguished as a sharp decrease in sea surface temperature (Rintoul et al., 2001; AnilKumar et al., 2006). The latitudinal migration of STF affects transport of water from the southwestern Indian Ocean to the Atlantic Ocean by the Agulhas Current (Flores et al., 1999). The response of ARC to the changes in the hydrography of the southwestern Indian Ocean over the glacial–interglacial time scales is not clear yet.

The physico-chemical state of the southwestern Indian Ocean is also an important component of the monsoon system and modulates the intensity and timing of monsoon in India (Clemens et al., 1991), as well as African region (Bader and Latif, 2003). Any change in global climate will affect the thermal structure of the southwestern Indian Ocean which in turn may act as feedback for further climate change. Therefore it is

CPD
9, 5521–5551, 2013

necessary to understand hydrographic changes in the southwestern Indian Ocean during the last glacial–interglacial transition, which will help to constrain the past climatic history of both the Indian monsoon as well the southeastern Atlantic Ocean. Limited information is available on past climatic history of the southwestern Indian Ocean. Therefore, here we have used changes in abundance, stable isotopic ratio ($\delta^{18}O$) and trace metal ratio (Mg/Ca) of planktic foraminifer *Globigerina bulloides* foraminifera, along with the relative abundance of *Neogloboquadrina pachyderma* Dextral to reconstruct paleoclimatic changes from the southwestern Indian Ocean, with an aim to understand changes in the strength of ARC over the last glacial–interglacial cycle.

Globigerina bulloides is abundant during periods of high phytoplankton productivity (Schiebel et al., 1997). It has wide temperature tolerance limit and has been reported from almost all possible sea surface temperature range in the world oceans (Bé and Hutson, 1977; Hemleben et al., 1989; Sautter and Thunell, 1989). A several orders of magnitude higher abundance of *G. bulloides* is reported in the areas having high phytoplankton population, as a result of upwelling of nutrient rich cold water from deeper depths to the surface (Peeters et al., 2002). Recently, Záric et al. (2006) and Fraile et al. (2008) modeled the global distribution of planktic foraminiferal species including *G. bulloides* and found that this species is strongly correlated with highly productive regions. High productivity regions in the Indian Ocean are generally associated with upwelling induced by seasonal strong winds (Wyrtki, 1971; McCreary et al., 1996; Naidu et al., 1999). Thus the temporal variation in the relative abundance of *G. bulloides* in the Indian Ocean region has been suggested as an efficient tracer for the past changes in the surface productivity as a result of wind-driven upwelling associated with summer monsoon (Prell and Curry, 1981; Naidu et al., 1999). A surface to near surface habitat for *G. bulloides* in the Southern Ocean was inferred based on $\delta^{18}O$ of the specimens collected in sediment traps (King and Howard, 2005). In view of reported increased abundance of *G. bulloides* in waters with high surface productivity, it has been widely used to infer paleo-upwelling and thus paleomonsoon changes in the Indian Ocean region (Naidu et al., 1999; Gupta et al., 2003). Increased relative abundance of *Neogloboquadrina pachyderma* (dex.) is also reported in upwelling areas including that around 40° S, though the effect of seawater temperature was also observed (Záric et al., 2006; Fraile et al., 2008).

2 The study area

The core was collected from the ARR and falls in the path of ARC in the southwestern Indian Ocean which is characterized by a subtropical anticyclonic gyre (Stramma and Lutjeharms, 1997). The westward-flowing South Equatorial Current (SEC) between 10–20° S, is the gyre's northern boundary (Schott et al., 2009). The Madagascar bifurcates the westward flowing SEC into the Mozambique Channel and the East Madagascar Current (EMC). The African subcontinent further deflects the SEC pole-ward as the Agulhas Current until a part of it, the ARC, joins the eastward-flowing Antarctic Circumpolar Current (ACC) and then completes the loop by flowing equator-ward as the West Australian Current (Read and Pollard, 1993; de Ruijter et al., 2005). The Agulhas Current frequently sheds rings as a result of retroflection (Schouten et al., 2000). These rings carry warm and salty Indian Ocean water into the South Atlantic (de Ruijter et al., 1999). The Agulhas Current transports ~ 70 Sv of water, with contributions of 18 Sv and 20 Sv from the Mozambique Channel and the East Madagascar Current, respectively (Donohue and Toole, 2003). Stramma (1992) identified the South Indian Ocean Current (SOC) lying at or near the Subtropical Front (STF) that is located at ~ 40° S in the central South Indian Ocean. The STF separates the warmer and saltier water of the subtropics from the cold, fresh, nutrient-rich subantarctic water. The region around the core is marked by year-round strong upwelling due to interaction between EMC, Madagascar Ridge and local wind (Tomczak and Godfrey, 1994; Quartly et al., 2006; Poulton et al., 2009) as well as the factors associated with the Antarctic Circumpolar productivity belt (Ito et al., 2005).

The SEC, mainly sourced from the Indonesian Throughflow and Equatorial Counter Current (ECC), comprises the surface waters in the equatorial and southern part of the

CPD
9, 5521–5551, 2013

study area. A part of the northern region of the study area receives Equatorial Current surface waters that are partially derived from the Bay of Bengal region. Similarly, the southernmost part of the southwestern Indian Ocean receives surface waters from the subtropical gyre and subtropical current, which originate from the South Indian Ocean Current that flows north of the Circumpolar Current (Tomczak and Godfrey, 2003). Tritium data show that the Indonesian Throughflow contributes the large part of the Indian Ocean surface water north of 40° S and down to the thermocline (Fine, 1985).

The annual average sea surface temperature (SST) near the core location is 16.52 °C while the salinity (SSS) is 35.25. The minimum (14.23 °C) and maximum (18.87 °C) SST at the core location is reported during austral winter and summer seasons, respectively. The SST during other two seasons, i.e. spring (17.63 °C) and fall (16.17 °C), differs by ~ 1.5 °C. As compared to SST, small change (0.4 su) is observed in the surface seawater salinity, with the maximum SSS (35.4) reported during austral summer.

3 Materials and methodology

A total of 120 samples from the top 1.2 m section of a gravity core (SK 200/17, hereafter referred to as SWIOC) collected from 39.03° S latitude and 44.97° E longitude, at a water depth of 4022 m were used for this study (Fig. 1). The SWIOC was collected from the southwest Indian Ridge near Indome Fracture Zone, at the northern boundary of modern high productivity belt. The prominent topographic features surrounding this place include Agulhas basin on the west, Mozambique basin on the north west, Madagascar Basin on the northeast, Crozet Basin on the east and Crozet Ridge on the south. The core was collected as part of the "Pilot Expedition to the Southern Ocean" under the initiative of National Centre for Antarctic and Ocean Research, Goa.

An appropriate amount (5–10 g) of sample was collected in pre-weighed and properly labeled petri dishes and oven dried at 45–60 °C. The dried sample was weighed and soaked in water for a minimum of 24 h. The overlying water was decanted after 24 h.

CPD
9, 5521–5551, 2013

The procedure was repeated several times till the overlying water became clear. The sediment sample was then washed by using a 63 µm sieve using a very slow shower so as to prevent foraminiferal test breakage. The plus 63 µm fraction was then transferred in to small beakers for drying. The dried > 63 µm fraction was weighed and stored in plastic vials. The dried > 63 µm fraction was dry sieved using a 150 µm sieve. The > 150 µm fraction was used for picking planktic foraminifera. An appropriate amount of > 150 µm sand fraction was taken after coning and quartering. This representative fraction, so obtained, was weighed and uniformly spread over a gridded picking tray. From the representative fraction, all the planktic foraminiferal specimens were picked. From each sample, a minimum of ~ 300 specimens of planktic foraminifera were picked and mounted on micropaleontological slides. Out of the picked planktic foraminifera, all the specimens of *G. bulloides* were separated and counted by using "OLYMPUS SZX16" high-end research stereo microscope.

For stable oxygen isotopic analysis, 15–20 clean specimens of *G. bulloides* from 250–355 µm size range were picked. The specimens were gently crushed to break-open all the chambers and washed with ultra-pure water followed by methanol in 500 µL centrifuge tubes to remove clay and other extraneous material trapped inside the chambers. The cleaned fragments were transferred in to glass vials for measurement in the mass spectrometer. The stable isotopic ($\delta^{18}O$) ratio was measured at the National Institute of Oceanography, Goa, India using "Thermo Finnigan isotope ratio mass spectrometer" calibrated via NBS 18 to the PDB scale. The values are given in δ-notation vs. VPDB (Vienna Pee Dee Belemnite). The precision of oxygen isotope measurements based on repeat analyses of NBS 18 and a laboratory standard runs over a long period was better than 0.1 ‰. For elemental (Mg/Ca) analysis, ~ 25–30 clean specimens of *G. bulloides* from 250–355 µm size range were picked, weighed, crushed and transferred to plastic centrifuge tubes. The specimens were cleaned following the UCSB standard foraminifera cleaning procedure without the DTPA step (Martin and Lea, 2002). Thoroughly cleaned samples were analyzed by using a Thermo Finnigan Element2 sector field ICP-MS following the isotope dilution/internal standard method

CPD
9, 5521–5551, 2013

(Martin and Lea, 2002). The *G. bulloides* Mg/Ca ratio was converted to SST by using the calibration equation of Mashiotta et al. (1999).

$$Mg/Ca = 0.474(\exp 0.107 Temp)$$

The error in Mg/Ca seawater temperature is ±0.8 °C, based on the error associated with the calibration equation. The planktic foraminiferal Mg/Ca ratio indicates the seawater temperature while $\delta^{18}O$ depends on both the seawater temperature and the oxygen isotopic ratio of the seawater. In order to assess the possible dissolution effect on foraminiferal Mg/Ca ratio, the shell weight was measured prior to crushing the tests for trace metal analysis. The stable isotopic and trace metal data of SWIOC is compared with another core (RC11-120) collected from the same latitude but more easterly longitude (Mashiotta et al., 1999).

4 Chronology of the core

The $\delta^{18}O$ *G. bulloides* from this core was compared with low latitude planktic foraminiferal global isostack (Bassinot et al., 1994) and cross-checked with $\delta^{18}O$ benthic foraminiferal global isostack of Lisiecki and Raymo (2005) to determine the tie points to establish the chronology (Fig. 2). A total of 7 tie-points corresponding with Marine Isotopic Stage (MIS) 2.2, 3, 4 and 5 and sub-stage 5.2, 5.4 and 5.5 were used to establish the chronology. The sedimentation rate varies from a minimum of 0.3 cm kyr^{-1} between 17–24 kyr and 86–106 kyr to a maximum of 3.6 cm kyr^{-1} between ∼ 9 kyr to 17 kyr (average 1.1 cm kyr^{-1}). The core top age could not be determined due to unavailability of sufficient number of intact planktic foraminiferal tests. The next section with sufficient shells available for dating was 9–10 cm which was radiocarbon dated to be 8600 ± 300 yr old. The dating was carried out at the Accelerator Mass Spectrometer facility of the Institute of Physics, Bhubneshwar, India. The chronology of the top 10 cm section was interpolated based on the sedimentation rate between 9–10 cm section and the age of MIS 2.2 taken as 17 kyr.

5 Results

The analyzed section covers a time-span of 150 kyr at an average sample resolution of ~1 kyr. The core-top is 7 kyr old suggesting a loss of top several cm of the sediments during coring. The fraction > 63 µm increased during the early part of MIS6 covered by the studied section and decreased to its lowest reported value throughout the core towards the MIS6/5 transition (Fig. 3). The fraction > 63 µm almost entirely consists of planktic foraminiferal tests and its fragments. A gradual increase in both the planktic foraminiferal abundance and fraction > 63 µm is noted during MIS5. A gradual increase is also noted in the *G. bulloides* relative abundance during MIS5. The δ^{18}O *G. bulloides* though initially gets depleted from the bottom of the section till MIS5.5, subsequently becomes heavier till the MIS5/4 transition. The relative abundance of *N. pachyderma* dextral also increases during early part of MIS5, but remains constant from ~ 80 kyr onwards till MIS5/4 transition. The Mg/Ca also increases during early part of the MIS5 till MIS5/4 transition.

As compared to MIS5, the planktic foraminiferal abundance as well as the percentage of fraction > 63 µm do not show large variation during MIS4. The planktic foraminiferal abundance and fraction > 63 µm during MIS4 are however higher than that during MIS5. The *G. bulloides* relative abundance increases abruptly from the early MIS4 to late MIS4. A distinct enrichment of δ^{18}O *G. bulloides* is noticed during MIS4. The *N. pachyderma* relative abundance remains unchanged throughout the MIS4 only to increase abruptly towards MIS4/3 transition. Decrease in Mg/Ca based seawater temperature is also observed during late MIS4 (Fig. 3).

No significant change is noted in planktic foraminiferal abundance, fraction > 63 µm and *N. pachyderma* relative abundance during the early MIS3. The planktic foraminiferal abundance and fraction > 63 µm increase from ~ 40 kyr onwards till the MIS3/2 transition. The *G. bulloides* relative abundance decreases throughout the MIS3 to reach to a level towards the MIS3/2 transition which is comparable with early MIS5. The δ^{18}O *G. bulloides*, however gets enriched from 40 kyr to LGM corresponding to

17 kyr. The *N. pachyderma* relative abundance decreases during this interval, only to increase from ~ 35 kyr BP till the MIS3/2 transition. A decrease in Mg/Ca seawater temperature is noted from MIS4/3 transition till MIS3/2 transition. The highest planktic foraminiferal abundance and fraction > 63 µm, is noted during MIS3/2 transition whereas the *G. bulloides* relative abundance is at its lowest during this period.

During MIS2, both planktic foraminiferal abundance and fraction > 63 µm decrease abruptly whereas Mg/Ca seawater temperature and *G. bulloides* relative abundance increase. The $\delta^{18}O$ *G. bulloides* gets further depleted during the early part of MIS2. As compared to the rest of the parameters, minor fluctuations are noted in *N. pachyderma* relative abundance during early MIS 2, with a net increase, during the late MIS2. The highest *N. pachyderma* relative abundance however is noted during late MIS 2. The Mg/Ca seawater temperature also increases from 20 kyr onwards till MIS 2/1 transition. The planktic foraminiferal abundance, fraction > 63 µm and Mg/Ca seawater temperature increase during early Holocene, whereas the *G. bulloides* relative abundance and *N. pachyderma* relative abundance decrease during early Holocene. The $\delta^{18}O$ *G. bulloides* gets further depleted during early Holocene.

A decrease in *G. bulloides* shell weight is observed during the MIS5. The shell weight increases from late MIS5 and throughout MIS 4 till early MIS3. During MIS3, shell weight remains constant with minor variations. The shell weight decreases during early MIS2 followed by an increase till MIS 2/1 transition. A decrease in shell weight is observed during the early Holocene.

The LGM (taken as the average of 5 most depleted intervals centered at 17 kyr) early Holocene difference in $\delta^{18}O$ *G. bulloides* is ~ 1.45 ± 0.6 ‰. The core-top Mg/Ca SST is 8.8 °C (1.21 mmol mol^{-1} Mg/Ca), much lower than the average austral spring SST (~ 14.5 °C) in the area. The LGM-Holocene difference in Mg/Ca seawater temperature is 1.2 ± 1.2 °C. The lowest Mg/Ca seawater temperature (6.5 °C) at 21.2 kyr BP), however is ~ 3 °C cooler than the average early Holocene Mg/Ca SST (9.5 ± 0.8 °C). This lowest LGM Mg/Ca seawater temperature, however is ~ 8 °C lower than the average spring SST near the core-site.

6 Discussion

6.1 Reliability of faunal data: comparison with previous work

The average *G. bulloides* relative abundance during early Holocene, in our core (6 ± 2 %) is lower than that in the plankton tow (10.0–19.9 %) and surface sediment samples (20.0–49.9 %) reported previously from the southwestern Indian Ocean (Bé and Hutson, 1977; Fraile et al., 2009). The abundance of *G. bulloides* is also lower than that at a southwesterly site wherein it comprises 20–30 % of the planktic foraminiferal population in the sediments, whereas in the sediment traps, it constitutes upto 19–24 % of the total planktic foraminifera, next only to *N. pachyderma* (King and Howard, 2003). The difference probably reflects the high spatial variability in the relative abundance of *G. bulloides* in this region as evident from very closely spaced *G. bulloides* abundance contours around the core site (Bé and Hutson, 1977; Fraile et al., 2009). The average *N. pachyderma* Dextral relative abundance in the Holocene section of our core (15 ± 3 %), however, is higher than its relative abundance in the plankton tows (0.1–4.9 %), but lower than that in the surface sediments (20.0–49.9 %) reported previously from this region (Bé and Hutson, 1977; Fraile et al., 2009). The difference in *N. pachyderma* abundance in the Holocene section of our core as compared to its relative abundance in the plankton tows probably reflects the seasonality associated with the plankton tows. A relatively higher abundance of *N. pachyderma* in a season other than the time when the plankton tows were collected will result in its higher relative abundance in surface sediments as the surface sediments contain the foraminiferal assemblage accumulated over a long time period as compared to the snapshot seasonal nature of plankton tows.

The early Holocene average $\delta^{18}O$ *G. bulloides* in our core (2.1 ± 0.4 ‰) is same as that in RC11-120 (2.2 ± 0.3 ‰) collected from comparable latitudes in the southeastern Indian Ocean. The average LGM $\delta^{18}O$ *G. bulloides* in our core (3.5 ± 0.5 ‰), also matches with that in RC11-120 (3.4 ± 0.1 ‰) (Mashiotta et al., 1999). The minor difference in average Holocene $\delta^{18}O$ *G. bulloides* at these two locations (0.1 ‰) partially

CPD
9, 5521–5551, 2013

reflects the lack of younger Holocene section in our core which might have still more depleted δ^{18}O.

The temperature dependent replacement of Ca by Mg in both inorganically (Chave, 1954; Katz, 1973; Oomori et al., 1987) and organically precipitated carbonates (Lea et al., 1999; Rosenthal et al., 2000; Barker et al., 2005) lead to the application of Mg/Ca ratio of foraminiferal shells as seawater temperature proxy. The Mg–Ca content of foraminiferal tests is however altered by post-depositional dissolution (Brown and Elderfield, 1996) for which measures have been suggested to estimate temperature, after correcting for dissolution-induced changes (Rosenthal and Lohmann, 2002). The early Holocene average Mg/Ca *G. bulloides* in our core (1.31 ± 0.11 mmol mol^{-1}) is lower than that in RC11-120 (1.60 ± 0.07 mmol mol^{-1}). The LGM average Mg/Ca in our core (1.16 ± 0.11 µmol mol^{-1}) is however comparable with that in RC11-120 (1.10 ± 0.07 ‰). The lower average Holocene Mg/Ca values in our core as compared to RC11-120, once again can be attributed to the lack of younger Holocene section in our core. Another possible cause for this difference might be dissolution as it affects foraminiferal Mg/Ca ratio (McCorkle et al., 1995; Brown and Elderfield, 1996; Rosenthal et al., 2000; Regenberg et al., 2006). It is possible that *G. bulloides* Mg/Ca at the core site is affected by partial dissolution as the core site lies below the modern carbonate saturation horizon. The modern carbonate saturation horizon in all three sectors of the Southern Ocean lies at ~ 3400 m water depth (Howard and Prell, 1994). Increased carbonate dissolution during glacial periods is also reported from the Indian sector of the Southern Ocean. The cores recovered from the Cape Basin reveal that the carbonate saturation horizon during MIS 2 and 4 was ~ 600 m shallower than present (Howard and Prell, 1994). A dissolution related bias in Mg/Ca *G. bulloides* can be assessed by comparing it with change in shell weight. The weight of individual *G. bulloides* shells varies from 12 µg during early part of MIS5 to 24 µg during MIS2. The shell weight increases throughout MIS4 through MIS3. This trend in *G. bulloides* shell weight does not correspond with its Mg/Ca, which has no significant variation during this interval. Even at a later interval (~ 15 kyr till core-top), while the shell weight decreases, the Mg/Ca

CPD
9, 5521–5551, 2013

Title Page
Abstract | Introduction
Conclusions | References
Tables | Figures
◄| |►
◄ ►
Back | Close
Full Screen / Esc
Printer-friendly Version
Interactive Discussion

increases. Non-corresponding variation in *G. bulloides* shell weight and its Mg/Ca ratio suggest that changes in Mg/Ca at our core-site are possibly not hugely affected by dissolution.

6.2 Productivity changes: Southern Ocean as atmospheric CO_2 regulator

As compared to early Holocene, a high relative abundance of *G. bulloides* throughout the last glacial period especially during MIS 4 and 2, suggests high productivity in the southwestern Indian Ocean during cold periods. Several studies have suggested increased productivity in the region north of subantarctic zone of the Southern Ocean during glacial period (Sigman and Boyle, 2000; Jaccard et al., 2013). The high productivity in this region is likely related to the enhanced availability of nutrients as a result of equatorward shift of westerlies as suggested by Toggweiler et al. (2006) based on modeling studies. The strengthening of Southern Hemisphere westerlies between 36° S and 43° S during glacial period as compared to interglacial was also inferred by Shulmeister et al. (2004) based on a synthesis of a large number of paleodata. The exact nature of Southern Hemisphere westerlies during glacial periods, however is debated (Chavaillaz et al., 2013; Sime et al., 2013). A minor northward shift in hydrographic regime in this region will affect faunal abundance as *G. bulloides* comprise the major component of subpolar assemblage which dominates between 40° S and 53° S latitudes (Howard and Prell, 1984). Further, the *G. bulloides* abundance increases during austral spring season, suggesting factors like shallow mixed layer depth and nutrient availability as evident from increased chlorophyll concentration, other than temperature as control on its distribution. The $\delta^{18}O$ *G. bulloides* from sediment traps deployed in the southwestern Indian Ocean and Southern Ocean suggest that this species lives in the surface waters during the austral spring season (King and Howard, 2005), though the depth of maximum abundance varies with latitudes (Mortyn and Charles, 2003). Sediment trap and plankton tow studies further suggest that *G. bulloides* though can tolerate wide range of seawater temperature (5–20 °C), its peak abundance is almost always associated with a chlorophyll maximum during periods of high phytoplankton produc-

CPD
9, 5521–5551, 2013
Migrating subtropical front and Agulhas Return Current
D. K. Naik et al.

tivity (Fairbanks et al., 1982; Thunell and Reynolds, 1984; Reynolds and Thunell, 1985; Sautter and Thunell, 1989, 1991; Ortiz et al., 1995; King and Howard, 2003). The high productivity during cold periods as inferred from *G. bulloides* relative abundance is further supported by increased abundance of *N. pachyderma* Dextral. A difference in relative abundance of *N. pachyderma* Dextral and *G. bulloides* is however noted and is attributed to the difference in timing of change in seawater temperature and productivity and is discussed in the next section. The glacial high productivity events as indicated by *G. bulloides* relative abundance confirm previous assumptions about a dominant control of the Southern Ocean on glacial–interglacial change in atmospheric CO_2.

6.3 Difference in *G. bulloides* and *N. pachyderma* abundance: water column structure and migrating STF

The unique feature of our record is an abrupt increase in *G. bulloides* relative abundance during MIS 4 as well as MIS2, indicating high productivity events. The later part of both of these high *G. bulloides* relative abundance events however also coincides with an increase in abundance of *N. pachyderma* Dextral. The peak abundance of *N. pachyderma* Dextral is strongly associated with both the pycnocline depth in the Southern Ocean which is most likely controlled by the thermocline as well as productivity (Mortyn and Charles, 2003) suggesting that a part of the high productivity events in the southwestern Indian Ocean during cold periods is associated with warming as *N. pachyderma* peak flux, in this region is observed during austral summer (King and Howard, 2005). A part of this warming was, also accompanied by a corresponding increase in *G. bulloides* Mg/Ca, suggesting warming of entire water column. The concurrent increase in relative abundance of both *G. bulloides* and *N. pachyderma* Dextral, further suggests strong thermocline. It implies that the nutrients for the high productivity events as inferred from *G. bulloides* relative abundance were not only supplied by the upwelled water, rather it also suggests the role of either the windblown dust or ice-rafted debris. The year-long upwelling would have dissipated the thermocline which should result in decreased *N. pachyderma* relative abundance. The possibility

CPD
9, 5521–5551, 2013

of seasonal high productivity and strong thermocline, however is not ruled out as it is beyond the scope of this work. The strong winds would also result in deeper mixed layer and increased nutrient availability which is reflected in high *N. pachyderma* relative abundance. This evidence that warming was more pronounced in and most likely confined to the sub-surface waters, confirms the model studies wherein it is found that the non-breaking surface wave-induced mixing in the Southern Ocean can reduce sea surface temperature and increase subsurface temperature of the upper ocean (Huang et al., 2012).

The increased abundance of *N. pachyderma* Dextral only in the later part of MIS 4 and 2 suggests that a critical point was reached during this time, when the STF moved to such a northerly position that it helped to force early retroflection of Agulhas Current, thus bringing warm and salty water to the core location. The average position of the Subantarctic Front at the LGM (LGM-SAF) was at 43° S (Brathauer and Abelmann, 1999; Gersonde et al., 2003, 2005). This work further suggests that during LGM the position of STF was more northerly than that off the southern tip of Africa wherein it was same as that at present (Gersonde et al., 2003). Earlier, Bé and Duplessy (1976) suggested that the northern limit of STF in the southwestern Indian Ocean during glacial period was upto 31° S. These findings were further confirmed by Bard and Rickaby (2009) who reported migration of STF to as far north as ~ 33° S in this region based on faunal and sediment characteristics in core MD962077, which was collected from the southwestern Indian Ocean.

A change in *G. bulloides* abundance in SWIOC can be interpreted as migration of high productivity belt centered at the southern boundary of STF and northern boundary of SAF, whereas variations in abundance of *N. pachyderma* Dextral can be linked to the strength of ARC as it warm this regions. The beginning of significant increase in the abundance of *G. bulloides* prior to *N. pachyderma* thus suggests that the northward migration of STF preceded and probably forced easterly migration of Agulhas Retroflection. Increased interaction of warm and salty ARC water with the cold SAF waters over the core site might have lead to increased productivity observed as increased

CPD
9, 5521–5551, 2013

abundance of *G. bulloides*. Increased abundance of *G. bulloides* has been suggested as indicator of more austral spring season like condition (King and Howard, 2003). It would lead to more intense ARC as model simulations suggest that the circulation in the Agulhas Retroflection region strengthens during austral spring through summer in response to intense winds (Matano et al., 1999). Previously, increased productivity and low seawater temperatures during each glacial period were interpreted as northward migration of subtropical front further closing the Agulhas Current (Bard and Rickaby, 2009).

6.4 Subtle temperature salinity change: role of Agulhas retroflection current

The LGM-early Holocene Mg/Ca temperature difference in the southwestern Indian Ocean is only 1.2 ± 1.2 °C, which is lower than that in the southeastern Indian Ocean (3.5 ± 0.4 °C) (Mashiotta et al., 1999) (Fig. 4). The error here is calculated from the standard deviation of the average Mg/Ca temperature during the Holocene and LGM. This LGM-early Holocene SST difference is also lower than radiolarian based estimates which suggest that LGM summer sea surface temperature around the core site was ∼ 4–5 °C cooler as compared to modern SST (Gersonde et al., 2005). It should however be noted here that this small difference in temperature may partly reflect lack of complete Holocene section in SWIOC. The difference in LGM-early Holocene δ^{18}O *G. bulloides* 1.45 ± 0.6 ‰ in the southwestern Indian Ocean is, however larger than that in the southeastern Indian Ocean (1.23 ± 0.4 ‰). Considering average ice-volume contribution of 1.0 ± 0.1 % over the glacial–interglacial transition (Schrag et al., 2002) leaves 0.45 ± 0.6 ‰ δ^{18}O, which includes both temperature and salinity components. Removing temperature component (0.2 ‰ change per 1 °C change in temperature), results in 0.2 ‰ δ^{18}O which can be attributed to local salinity changes. We suggest that comparatively less cooling during the last glacial period in the southwestern Indian Ocean is due to the enhanced influence of ARC. Increased transport of subtropical warm water by ARC will warm the Agulhas Retroflection Region. Previous studies have also suggested that though the transport of warm and salty water from the In-

CPD
9, 5521–5551, 2013

dian to south Atlantic Ocean continued throughout the LGM, but with reduced intensity (Gersonde et al., 2003). The reduced Agulhas leakage was probably driven by increased wind stress in this region. Large wind stress amplitude can trigger turbulent regime, which decreases the availability of Indian Ocean water for the Agulhas leakage (Matano, 1996; Matano et al., 1999; Le Bars et al., 2012). Recently it was reported that high wind stress in the southwestern Indian Ocean decreases the rate or cessation of eddy shedding by the AC leading to increased retroflection and delayed transport of previously shed eddy further westward into the Atlantic Ocean and thus increases seawater temperature off the southern tip of Africa (van Aken et al., 2013). We suggest that early retroflection (in more easterly longitudes) during glacial period lead to increased transport of warm water in the ARR. An easterly shift in retroflection from at $\sim 15^{\circ}$ E during austral winter to $\sim 25^{\circ}$ E during summer is noticed at present. A weaker transport of the Agulhas Current during the winter months was suggested to cause westward shift of retroflection region (Matano et al., 1998). The early retroflection of ARC in more easterly latitudes during glacial period is further supported by previous studies suggesting increased influence of ARC (relatively warm and stratified surface waters) off the southern tip of Africa, a region which lies in the path of Agulhas Current and eddy shedding, during MIS 1 and 5 and decreased influence during MIS 2 and 4, as inferred from changes in coccolithophores (Flores et al., 1999). Peeters et al. (2004) also inferred enhanced Indian–Atlantic water exchange during present and last interglacial while reduced exchange during glacial periods. The region west off southern tip of Africa will show signatures of AC while the region east of it is influenced by ARC, thus recording opposite signals.

Though the Mg/Ca SST during the last glacial period prior to LGM was comparable with the early Holocene SST, we did not see a progressive increase in sea surface temperature during the glacial period as previously reported from the southwestern Indian Ocean (Martínez-Méndez et al., 2010). The δ^{18}O *G. bulloides* was depleted in the southwestern Indian Ocean as compared with the southeastern Indian Ocean throughout the last glacial period. The difference was more pronounced during MIS

CPD
9, 5521–5551, 2013

3. During the last glacial period, the difference in seawater temperature as estimated from *G. bulloides* Mg/Ca, however was smaller than that at present (6.5 °C). Additionally during MIS 2, the temperature of both of these regions was same. It further supports our hypothesis of early retroflection and strengthening of the Agulhas Return Current resulting in supply of warm water to the Indian sector of the Southern Ocean. The strengthened ARC warmed the entire Indian sector of the Southern Ocean, thus resulting in decreased longitudinal seawater temperature gradient. Therefore, we attribute the unique nature of our record to changes in the strength and position of ARC which drives the hydrology around the core-site.

7 Changes during Termination I

An interesting feature of this record is a drastic decline in *G. bulloides* abundance just prior to the last glacial maximum. The Mg/Ca temperature is also the lowest at this time, while $\delta^{18}O$ *G. bulloides* is yet to reach its most enriched LGM level. The recovery phase of *G. bulloides* relative abundance during early MIS 2 coincides with increase in Mg/Ca temperature. The peak *G. bulloides* relative abundance coincides with a peak in *N. pachyderma* relative abundance. The planktic foraminiferal abundance and fraction > 63 µm, however is at its lowest during this time. Both planktic foraminiferal abundance and fraction > 63 µm indicate either low productivity or a poor preservation of foraminiferal tests. The mid-transition increased *G. bulloides* abundance indicates increased surface productivity probably in response to the Antarctic Cold reversal. The decreased *G. bulloides* abundance during late deglaciation indicates decreased surface productivity probably due to melt-water lid induced increased stratification (Francois et al., 1993). As high *G. bulloides* relative abundance indicates increased productivity as discussed before, we suggest that the drop in planktic foraminiferal abundance and fraction > 63 µm during Termination I is the result of poor preservation. The variation in planktic foraminiferal abundance is similar to the change in carbonate percentage (higher during glacial period than during interglacial) observed in cores collected from the southeastern Atlantic off the southwestern coast of Africa (Hodell et al., 2001). A sharp decrease in both the planktic foraminiferal abundance as well as fraction > 63 µm during termination, indicates sharp decline in carbonate percentage during termination which is a characteristic of cores collected from this region.

8 Conclusions

Based on the faunal, stable isotopic and trace metal analysis of planktic foraminifera in a core collected from the southwestern Indian Ocean in the path of Agulhas Retroflection Current, we infer that over the last glacial–interglacial cycle, the hydrography of this region was driven by change in the position of retroflection region as well as migrating subtropical front. The productivity in the southwestern Indian Ocean increased during cold periods which confirm previous reports. The increased productivity during glacial period suggests northward migration of subtropical front. The increased relative abundance of *N. pachyderma* Dextral is inferred as a result of strong thermocline due to eastward shifting of ARR which brings warmer and saltier water to the southwestern Indian Ocean. The findings confirm previous reports of Southern Ocean as the store-house of atmospheric carbon during glacial period.

Acknowledgements. Authors are thankful to the Director, National Institute of Oceanography and National center for Antarctic and Ocean Research for providing the facility to carry out the work. We express our sincere thanks to Rahul Mohan, Program Director, Antarctic Science, of NCAOR, Goa for providing all support for this work. V. K. Banakar and Ms. Anita Garg of NIO, Goa is thankfully acknowledged for the stable oxygen isotopic measurements. The help of David Lea and Georges Paradis of University of California, Santa Barbara in analyzing the trace metal ratio is sincerely acknowledged. This work is a part of the project funded by NCAOR Goa, India. The help of Sujata Kurtarkar in picking foraminiferal specimens is thankfully acknowledged.

CPD
9, 5521–5551, 2013

References

Anilkumar, N., Luis, A. J., Somayajulu, Y. K., Ramesh Babu, V. M., Dash, K., Pednekar, S. M., Babu, K. N., Sudhakar, M., and Pandey, P. C.: Fronts, water masses and heat content variability in the Western Indian sector of the Southern Ocean during austral summer 2004, J. Marine Syst., 63, 20–34, 2006.

Bader, J. and Latif, M.: The impact of decadal-scale Indian Ocean sea surface temperature anomalies on Sahelian rainfall and the North Atlantic Oscillation, Geophys. Res. Lett., 30, 2169, doi:10.1029/2003GL018426, 2003.

Bard, E. and Rickaby, R. E. M.: Migration of the subtropical front as a modulator of glacial climate, Nature, 460, 380–383, 2009.

Barker, S., Cacho, I., Benway, H., and Tachikawa, K.: Planktonic foraminiferal Mg / Ca as a proxy for past oceanic temperatures: a methodological overview and data compilation for the Last Glacial Maximum, Quaternary Sci. Rev., 24, 821–834, 2005.

Barker, S., Diz, P., Vautravers, M. J., Pike, J., Knorr, G., Hall, I. R., and Broecker, W. S.: Interhemispheric Atlantic seesaw response during the last deglaciation, Nature, 457, 1097–1102, 2009.

Bassinot, F. C., Labeyrie, L. D., Vincent, E. X. Q., Shackleton, N. J., and Lancelot, Y.: The astronomical theory of climate and the age of the Brunhes-Matuyama magnetic reversal, Earth Planet. Sci. Lett., 126, 91–108, 1994.

Bé, A. W. H. and Duplessy, J. C.: Subtropical convergence fluctuations and quaternary climates in the middle latitudes of the Indian Ocean, Science, 194, 419–422, 1976.

Bé, A. W. H. and Hutson, W. H.: Ecology of planktonic foraminifera and biogeographic patterns of life and fossil assemblages in the Indian Ocean, Micropaleontology, 23, 369– 414, 1977.

Beal, L. M., De Ruijter, W. P. M., Biastoch, A., Zahn, R., and SCOR/WCRP/IAPSO Working Group: On the role of the Agulhas system in ocean circulation and climate, Nature, 472, 429–436, 2011.

Brathauer, U. and Abelmann, A.: Late Quaternary variations in sea surface temperatures and their relationship to orbital forcing recorded in the Southern Ocean (Atlantic sector), Paleoceanography, 14, 135–148, 1999.

Brown, S. J. and Elderfield, H.: Variations in Mg / Ca and Sr / Ca ratios of planktonic foraminifera caused by postdepositional dissolution: evidence of a shallow Mg-dependent dissolution, Paleoceanography, 11, 543–551, 1996.

CPD
9, 5521–5551, 2013

Migrating subtropical front and Agulhas Return Current

D. K. Naik et al.

Bryden, H. L. and Beal, L. M.: Role of the Agulhas Current in Indian Ocean circulation and associated heat and freshwater fluxes, Deep-Sea Res. I, 48, 1821–1845, 2001.
Chavaillaz, Y., Codron, F., and Kageyama, M.: Southern westerlies in LGM and future (RCP4.5) climates, Clim. Past, 9, 517–524, doi:10.5194/cp-9-517-2013, 2013.
Chave, K. E.: Aspects of the biogeochemistry of magnesium 1. Calcareous marine organisms, J. Geol., 62, 266–283, 1954.
Clemens, S. C., Prell, W. L., Murray, D., Shimmield, G., and Weedon, G.: Forcing mechanisms of the Indian Ocean monsoon, Nature, 353, 720–725, 1991.
de Ruijter, W. P. M., Biastoch, A., Drijfhout, S. S., Lutjeharms, J. R. E., Matano, R. P., Pichevin, T., van Leeuwen, P. J., and Weijer, W.: Indian-Atlantic interocean exchange: dynamics, estimation and impact, J. Geophys. Res., 104, 20885–20910, 1999.
de Ruijter, W. P. M., Ridderinkhof, H., and Schouten, M. W.: Variability of the southwest Indian Ocean, Phil. Trans. R. Soc. A,363, 63–76, 2005.
Donohue, K. A. and Toole, J.: A near-synoptic survey of the Southwest Indian Ocean, Deep-Sea Res., 50, 1893–1931, 2003.
Fairbanks, R. G., Sverdlove, M. S., Free, R., Wiebe, P. H., and Bé, A. W. H.: Vertical distribution and isotopic fractionation of living planktonic foraminifera from the Panama Basin, Nature, 298, 841–844, 1982.
Fine, R. A.: Direct evidence using tritium data for throughflow from the Pacific into the Indian Ocean, Nature, 315, 478–480, 1985.
Flores, J. A., Gersonde, R., and Sierro, F. J.: Pleistocene fluctuations in the Agulhas Current Retroflection based on the calcareous plankton record, Mar. Micropaleontol., 37, 1–22, 1999.
Fraile, I., Schulz, M., Mulitza, S., and Kucera, M.: Predicting the global distribution of planktonic foraminifera using a dynamic ecosystem model, Biogeosciences, 5, 891–911, doi:10.5194/bg-5-891-2008, 2008.
Fraile, I., Schulz, M., Mulitza, S., Merkel, U., Prange, M., and Paul, A.: Modeling the seasonal distribution of planktonic foraminifera during the Last Glacial Maximum, Paleoceanography, 24, PA2216, doi:10.1029/2008PA001686, 2009.
Francois, R., Bacon, M. P., Altabet, M. A., and Labeyrie, L. D.: Glacial/interglacial changes in sediment rain rate in the SW Indian Sector of subantarctic Waters as recorded by ^{230}Th, ^{231}Pa, U, and $\delta^{15}N$, Paleoceanography, 8, 611–629, doi:10.1029/93PA00784, 1993.

CPD
9, 5521–5551, 2013

Migrating subtropical front and Agulhas Return Current

D. K. Naik et al.

Gersonde, R., Abelmann, A., Brathauer, U., Becquey, S., Bianchi, C., Cortese, G., Grobe, H., Kuhn, G., Niebler, H.-S., Segl, M., Sieger, R., Zielinski, U., and Fütterer, D. K.: Last glacial sea surface temperatures and sea-ice extent in the Southern Ocean (Atlantic-Indian sector): a multiproxy approach, Paleoceanography, 18, 1061, doi:10.1029/2002PA000809, 2003.

Gersonde, R., Crosta, X., Abelmann, A., and Armand, L.: Sea-surface temperature and sea ice distribution of the Southern Ocean at the epilog Last Glacial Maximum – a circum-Antarctic view based on siliceous microfossil records, Quat. Sci. Rev., 24, 869–896, 2005.

Gupta, A. K., Anderson, D. M., and Overpeck, J. T.: Abrupt changes in the Asian southwest monsoon during the Holocene and their links to the North Atlantic Ocean, Nature, 421, 354–357, 2003.

Gordon, A. L.: Interocean exchange of thermocline water. J. Geophys. Res., 91, 5037–5046, 1986.

Hemleben, Ch., Spindler, M., and Anderson, O. R.: Modern Planktonic Foraminifera, Springer-Verlag, New York, USA, 363 pp., 1989.

Hodell, D. A., Charles, C. D., and Sierro, F. J.: Late Pleistocene evolution of the ocean's carbonate system, Earth Planet. Sci. Lett., 192, 109–124, 2001.

Howard W. R., and Prell, W. L. A.: Comparison of radiolarian and foraminiferal paleoecology in the Southern Indian Ocean: new evidence for the interhemispheric timing of climatic change, Quaternary Res., 21, 244–263, 1984.

Howard, W. R. and Prell, W. L.: Late Quaternary $CaCO_3$ production and preservation in the Southern Ocean: implications for oceanic and atmospheric carbon cycling, Paleoceanography, 9, 453–482, doi:10.1029/93PA03524, 1994.

Huang, C. J., Qiao, F., Shu, Q., and Song, Z.: Evaluating austral summer mixed-layer response to surface wave-induced mixing in the Southern Ocean, J. Geophys. Res., 117, C00J18, doi:10.1029/2012JC007892, 2012.

Ito, T., Parekh, P., Dutkiewicz, S., and Follows, M. J.: The Antarctic Circumpolar Productivity Belt, Geophys. Res. Lett., 32, L13604, doi:10.1029/2005GL023021, 2005.

Jaccard, S. L., Hayes, C. T., Martínez-García, A., Hodell, D. A., Anderson, R. F., Sigman, D. M., and Haug, G. H.: Two modes of change in Southern Ocean productivity over the past million years, Science, 339, 6126, 1419–1423, 2013.

Katz, A.: The interaction of magnesium with calcite during crystal growth at 25–90 °C and one atmosphere, Geochim. Cosmochim. Ac., 37, 1563–1586, 1973.

King, A. and Howard, W. R.: Planktonic foraminiferal flux seasonality in Subantarctic sediment traps: a test for paleoclimate reconstructions, Paleoceanography, 18, 1008, doi:10.1029/2002PA000839, 2003.
King, A. L. and Howard, W. R.: $\delta^{18}O$ seasonality of planktonic foraminifera from the Southern Ocean sediment traps: latitudinal gradients and implications for paleoclimate reconstructions, Mar. Micropal., 56, 1–24, 2005.
Knorr, G. and Lohmann, G.: Southern Ocean origin for the resumption of Atlantic thermohaline circulation during deglaciation, Nature, 424, 532–536, 2003.
Lea, D. W., Mashiotta, T. A., and Spero, H. J.: Controls on magnesium and strontium uptake in planktonic foraminifera determined by live culturing, Geochim. Cosmochim. Ac., 63, 2369–2379, 1999.
Le Bars, D., De Ruijter, W. P. M., and Dijkstra, H. A.: A new regime of the Agulhas current retroflection: turbulent choking of Indian-Atlantic leakage, J. Phys. Oceanogr., 42, 1158–1172, 2012.
Lisiecki, L. E. and Raymo, M. E.: A Pliocene-Pleistocene stack of 57 globally distributed benthic $\delta^{18}O$ records, Paleoceanography, 20, PA1003, doi:10.1029/2004PA001071, 2005.
Lutjeharms, J. R. E. and Ansorge, I. J.: The Agulhas return current, J. Marine Syst., 30, 115–138, 2001.
Lutjeharms, J. R. E. and van Ballegooyen, R. C.: The retroflection of the Agulhas current, J. Phys. Oceanogr., 18, 1570–1583, 1988.
Martin, P. A. and Lea, D. W.: A simple evaluation of cleaning procedures on fossil benthic foraminiferal Mg / Ca, Geochem. Geophy. Geosy., 3, 8401, doi:10.1029/2001GC000280, 2002.
Martínez-Méndez, G., Zahn, R., Hall, I. R., Peeters, F. J. C., Pena, L. D., Cacho, I., and Negre, C.: Contrasting multiproxy reconstructions of surface ocean hydrography in the Agulhas Corridor and implications for the Agulhas Leakage during the last 345 000 years, Paleoceanography, 25, PA4227, doi:10.1029/2009PA001879, 2010.
Mashiotta, T. A., Lea, D. W., and Spero, H. J.: Glacial–interglacial changes in Subantarctic sea surface temperature and d18O-water using foraminiferal Mg, Earth Planet Sc. Lett., 170, 417–432, 1999.
Matano, R. P.: A numerical study of the Agulhas retroflection: the role of bottom topography, J. Phys. Oceanogr., 26, 2267–2278, 1996.

CPD
9, 5521–5551, 2013

Migrating subtropical front and Agulhas Return Current

D. K. Naik et al.

Matano, R. P., Simionatoe, C. G., de Ruijter, W. P., van Leeuween, P. J., Strub, P. T., Chelton, D. B., and Schlax, M. G.: Seasonal variability in the Agulhas Retroflection region, Geophys. Res. Lett., 25, 4361–4364, 1998.
Matano, R. P., Simionato, C. G., and Strub, P. T.: Modeling the wind-driven variability of the south Indian Ocean, J. Phys. Oceanogr., 29, 217–230, 1999.
McCorkle, D. C., Martin, P. A., Lea, D. W., and Klinkhammer, G. P.: Evidence of a dissolution effect on benthic foraminiferal shell chemistry: $\delta^{13}C$, Cd / Ca, Ba / Ca and Sr / Ca from the Ontong Java Plateau, Paleoceanography, 10, 699–714, 1995.
McCreary, J. P., Kohler Jr., K. E., Hood, R. R., and Olson, D. B.: A four-component ecosystem model of biological activity in the Arabian Sea, Prog. Oceanogr., 37, 193–240, 1996.
Mortyn, P. G. and Charles, C. D.: Planktonic foraminiferal depth habitat and δ^{18}O calibrations: plankton tow results from the Atlantic sector of the Southern Ocean, Paleoceanography, 18, 1037, doi:10.1029/2001PA000637, 2003.
Naidu, P. D., Ramesh Kumar, M. R., and Ramesh Babu, V.: Time and space variations of monsoonal upwelling along the west and east coasts of India, Cont. Shelf Res., 19, 559–572, 1999.
Oomori, T., Kaneshima, H., and Maezato, Y.: Distribution coefficient of Mg^{2+} ions between calcite and solution at 10–50 °C, Mar. Chem., 20, 327–336, 1987.
Ortiz, J. D., Mix, A. C., and Collier, R. W.: Environmental control of living symbiotic and asymbiotic foraminifera of the California Current, Paleoceanography, 10, 987–1009, 1995.
Peeters, F. J. C., Brummer, G. J. A., Ganssen, G. M.: The effect of upwelling on the distribution and stable isotope composition of *Globigerina bulloides* and *Globigerinoides ruber* (planktic foraminifera) in modern surface waters of the NW Arabian Sea, Global Planet. Change, 34, 269–291, 2002.
Peeters, F. J. C., Acheson, R., Brummer, G. J. A., de Ruijter, W. P. M., Schneider, R. R., Ganssen, G. M., Ufkes, E., and Kroon, D.: Vigorous exchange between the Indian and Atlantic oceans at the end of the past five glacial periods, Nature, 430, 661–665, 2004.
Poulton, A. J., Stinchcombe, M. C., and Quartly, G. D.: High numbers of *Trichodesmium* and diazotrophic diatoms in the southwest Indian Ocean, Geophys. Res. Lett., 36, L15610, doi:10.1029/2009GL039719, 2009.
Prell, W. L. and Curry, W. B.: Faunal and isotopic indices of monsoonal upwelling: western Arabian Sea, Oceanol. Acta, 4, 91–98, 1981.

CPD
9, 5521–5551, 2013

Migrating subtropical front and Agulhas Return Current

D. K. Naik et al.

Title Page
Abstract | Introduction
Conclusions | References
Tables | Figures
◂◂ | ▸▸
◂ | ▸
Back | Close
Full Screen / Esc
Printer-friendly Version
Interactive Discussion

Quartly, G. D. and Srokosz, M. A.: Seasonal variations in the region of the Agulhas Retroflection: studies with Geosat and FRAM, J. Phys. Oceanogr., 23, 2107–2124, 1993.
Quartly, G. D., Buck, J. J. H., Srokosz, M. A., and Coward, A. C.: Eddies around Madagascar: the retroflection re-considered, J. Mar. Syst., 63, 115–129, 2006.
Rau, A. J., Rogers, J., Lutjeharms, J. R. E., Giraudeau, J., Lee-Thorp, J. A., Chen, M. T., and Waelbroeck, C.: A 450-kyr record of hydrological conditions on the western Agulhas Bank slope, south of Africa, Mar. Geol., 180, 183–201, 2002.
Read, J. F. and Pollard, R. T.: Structure and transport of Antarctic circumpolar current and Agulhas Return Current at 40° E, J. Geophys. Res., 98, 12281–12295, 1993.
Regenberg, M., Nürnberg, D., Steph, S., Groeneveld, J., Garbe-Schönberg, D., Tiedemann, R., and Dullo, W. C.: Assessing the effect of dissolution on planktonic foraminiferal Mg / Ca ratios: evidence from Caribbean core tops, Geochem. Geophy. Geosy., 7, Q07P15, doi:10.1029/2005GC001019, 2006.
Reynolds, L. A. and Thunell, R. C.: Seasonal succession of planktonic foraminifera in the subpolar North Pacific, J. Foramin. Res., 15, 282–301, 1985.
Rintoul, S. R., Hughes, C., and Olbers, D.: The Antarctic Circumpolar Current system, in: Ocean Circulation and Climate, edited by: Siedler, J. C. G. and Gould, J., Academic Press, Now York, 271–302, 2001.
Rosenthal, Y. and Lohmann, G. P.: Accurate estimation of sea surface temperatures using dissolution-corrected calibrations for Mg / Ca paleothermometry, Paleoceanography, 17, 1044, doi:10.1029/2001PA000749, 2002.
Rosenthal, Y., Lohman, G. P., Lohman, K. C., and Sherrell, R. M.: Incorporation and preservation of Mg in *Globigerinoides sacculifer*: implications for reconstructing the temperature and $^{18}O/^{16}O$ of seawater, Paleoceanography, 15, 135–145, 2000.
Sautter, L. R. and Thunell, R. C.: Seasonal succession of planktonic foraminifera: results from a four-year time-series sediment trap experiment in the northeast Pacific, J. Foramin. Res., 19, 253–267, 1989.
Sautter, L. R. and Thunell, R. C.: Planktonic foraminiferal response to upwelling and seasonal hydrographic conditions: sediment trap results from San Pedro Basin, Southern California Bight, J. Foramin. Res., 21, 347–363, 1991.
Schiebel, R., Bijma, J., Hemleben, C.: Population dynamics of the planktic foraminifer Globigerina bulloides from the eastern North Atlantic, Deep-Sea Res. Pt. I, 44, 1701–1713, 1997.

Schott, F. A., Xie, S. P., and McCreary Jr., J. P.: Indian Ocean circulation and climate variability, Rev. Geophys., 47, RG1002, doi:10.1029/2007RG000245, 2009.
Schouten, M. W., de Ruijter, W. P. M., van Leeuwen, P. J., and Lutjeharms, J. R. E.: Translation, decay and splitting of Agulhas rings in the south-east Atlantic Ocean, J. Geophys. Res., 105, 21913–21925, 2000.
Schrag, D. P., Adkins, J. F., McIntyre, K., Alexander, J. L., Hodell, D. A., Charles, C. D., and McManus, J. F.: The oxygen isotopic composition of seawater during the Last Glacial Maximum, Quaternary Sci. Rev., 21, 331–342, 2002.
Shulmeister, J., Goodwin, I., Renwick, J., Harle, K., Armand, L., McGlone, M. S., Cook, E., Dodson, J., Hesse, P. P., Mayewski, P., and Curran, M.: The Southern Hemisphere westerlies in the Australasian sector over the last glacial cycle: a synthesis, Quat. Int., 118–119, 23–53, 2004.
Sigman, D. M. and Boyle, E. A.: Glacial/interglacial variations in atmospheric carbon dioxide, Nature, 407, 859–869, 2000.
Sime, L. C., Kohfeld, K. E., Le Quéré, C., Wolff, E. W., de Boer, A. M., Graham, R. M., and Bopp, L.: Southern Hemisphere westerly wind changes during the Last Glacial Maximum: model-data comparison, Quat. Sci. Rev. 64, 104–120, 2013.
Stramma, L.: The South Indian Ocean current, J. Phys. Oceanogr., 22, 421–430, 1992.
Stramma, L. and Lutjeharms, J. R. E.: The flow of the subtropical gyre of the South Indian Ocean, J. Geophys. Res., 102, 5513–5530, 1997.
Toggweiler, J. R., Russell, J. L., and Carson, S. R.: Midlatitude westerlies, atmospheric CO_2, and climate change during the ice ages, Paleoceanography, 21, PA2005, doi:10.1029/2005PA001154, 2006.
Thunell, R. C. and Reynolds, L.: Sedimentation of planktonic foraminifera: seasonal changes in species flux in the Panama Basin, Micropaleontology, 30, 241–260, 1984.
Tomczak, M. and Godfrey, J. S.: Regional Oceanography: an Introduction, Pergamon, New York, 390 pp., 2003.
van Aken, H. M., Lutjeharms, J. R. E., Rouault, M., Whittle, C., and de Ruijter, W. P. M.: Observations of an early Agulhas Current Retroflection event in 2001: a temporary cessation of inter-ocean exchange south of Africa?, Deep-Sea Res. Pt. I, 72, 1–8, 2013.
Wyrtki, K.: Oceanographic Atlas of the International Indian Ocean Expedition, National Science Foundation, Washington, D.C., 531 pp., 1971.

Žarić, S., Schulz, M., and Mulitza, S.: Global prediction of planktic foraminiferal fluxes from hydrographic and productivity data, Biogeosciences, 3, 187–207, doi:10.5194/bg-3-187-2006, 2006.

CPD
9, 5521–5551, 2013

Migrating subtropical front and Agulhas Return Current

D. K. Naik et al.

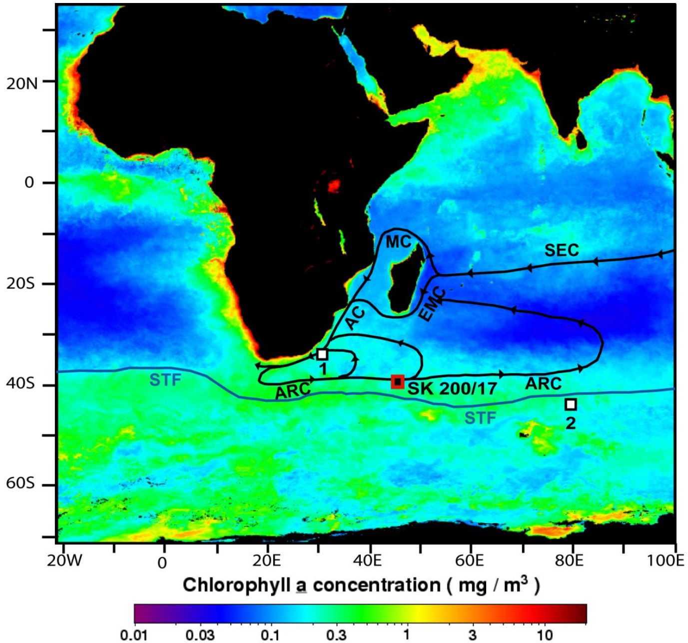

Fig. 1. The location of core SK 200/17 is marked with a black filled square. The surface circulation in this region, which includes South Equatorial Current (SEC), Mozambique Channel (MC), East Madagascar Current (EMC), Agulhas Current (AC) and Agulhas Retroflection/Return Current (ARC) is also marked. The position of subtropical front (STF) is marked with thick dark blue line. The other cores discussed in the text are also marked as 1 (MD962077, Bard and Rickaby, 2009) and 2 (RC11-120, Mashiotta et al., 1999). The template is the average productivity in terms of Chlorophyll a concentration in mg m^{-3}. The chlorophyll data was downloaded from OCEAN COLOR webpage (http://oceancolor.gsfc.nasa.gov/cgi/l3).

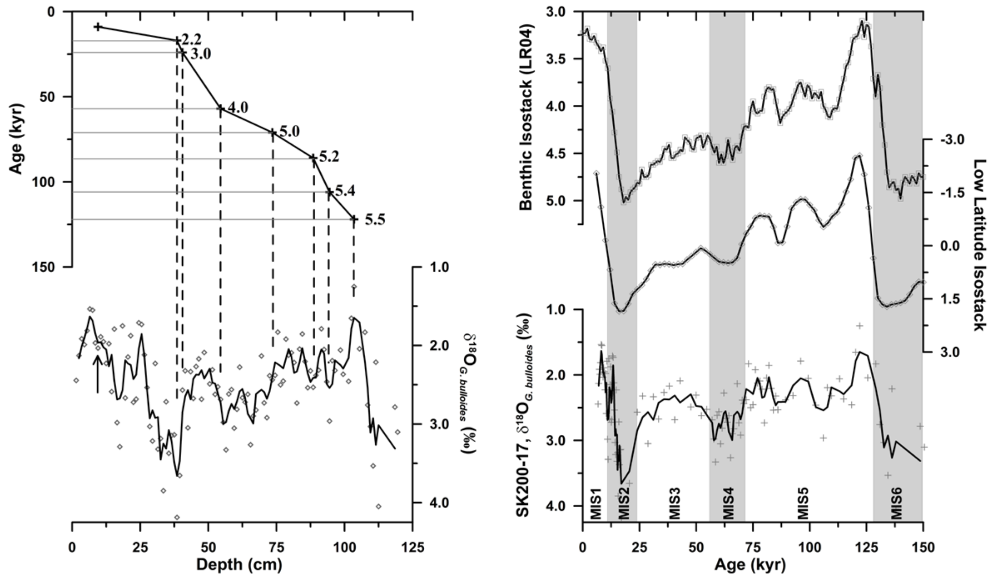

Fig. 2. The chronology of the core, as established by comparing the $\delta^{18}O$ *Globigerina bulloides* in the core with low latitude isostack map of Bassinot et al. (1994). This isostack curve was chosen as it is based on planktic foraminifera. The solid line represents three-point running average. The tie-point isotopic events are marked by dashed and light lines as well as the numbers. The single AMS date at 9–10 cm depth interval is marked by an arrow. The final chronology of core SK200/17 is compared with both low latitude isostack of Bassinot et al. (1994), as well as benthic foraminiferal isostack (LR04) of Lisiecki and Raymo (2005).

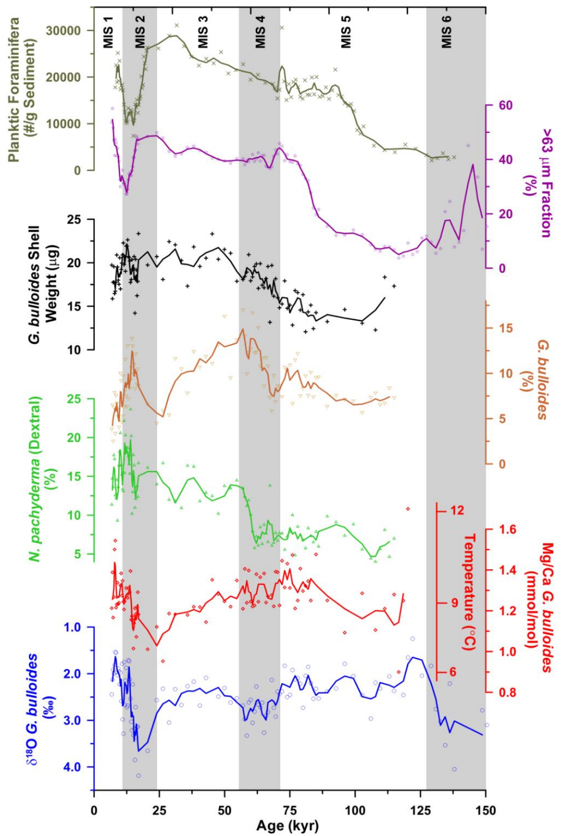

Fig. 3. Down-core variation in size fraction > 63 µm, planktic foraminiferal abundance (TPF g^{-1} Sediment), average *Globigerina bulloides* shell weight, relative abundance of *G. bulloides*, and *Neogloboquadrina pachyderma* Dextral, *G. bulloides* Mg/Ca along with estimated seawater temperature and δ^{18}O. The symbols are the actual values while the solid line is three-point running average.

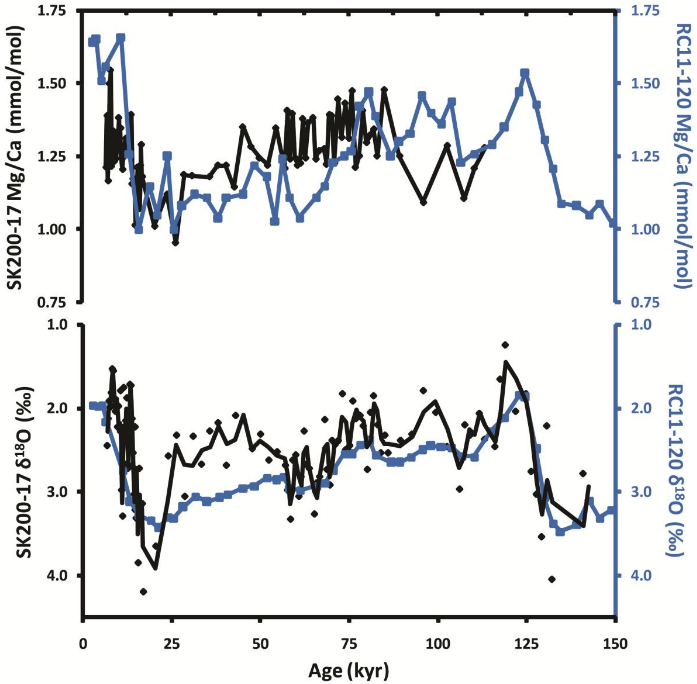

Fig. 4. A comparison of *Globigerina bulloides* δ^{18}O and Mg/Ca in core SK200/17 with that in RC11-120 which was collected from southeastern Indian Ocean (43°31′ S, 79°52′ E, 3135 m water depth, Mashiotta et al., 1999). The *G. bulloides* δ^{18}O of core SK200/17 is a three point running average.

CPD
9, 5521–5551, 2013